

Observation of Electron Trapping in a Positron Storage Ring

M.G. Billing, J. Conway, E.E. Cowan, J.A. Crittenden, J. Lanzoni, Y. Li, C.S. Shill, J.P. Sikora, and K.G. Sonnad
CLASSE, Cornell University, Ithaca, NY 14850, USA

Since 2008 the Cornell Electron Storage Ring has been investigating the feasibility and operational performance limits of low-emittance damping rings such as those required for the proposed International Linear Collider. Novel instrumentation including time-resolving electron detectors has been deployed in a wide variety of custom vacuum chambers and magnet types. Recently, measurements from such a detector installed in the field of a quadrupole magnet have shown clear evidence for long-term electron trapping. Based on modeling tuned to the measured signal, we conclude that about 5% of the electrons generated by a 10-bunch train of 5.3 GeV positrons with 14-ns spacing and 1.3×10^{11} population survive more than $2.5 \mu\text{s}$ in a quadrupole field of gradient 7.4 T/m.

One of the principle goals of Cornell Electron Storage Ring (CESR) Test Accelerator program, which has been underway since 2008, is to investigate the performance limitations of future high energy linear collider damping rings. These studies include measurements of electron cloud buildup caused by synchrotron radiation producing photoelectrons on the surface of the vacuum chamber. The CESR ring stores positron and electron beams of energy 1.8 GeV to 5.3 GeV arranged in bunches spaced in steps of 4 or 14 ns with bunch populations ranging up to 1.6×10^{11} . A variety of detectors sensitive to cloud electrons incident on the vacuum chamber wall have been brought into operation. Recently, a novel time-resolving electron detector installed in a quadrupole magnet has been commissioned. This Letter reports on measurements of electron trapping obtained with this detector.

Electron cloud buildup has been observed in many types of accelerators since the 1960s [2], and was an important factor in the operation of the storage rings KEK-B in Japan [3] and PEP-II in the U.S [4]. Typical decay times for electron clouds in the absence of magnetic trapping effects are about 100 ns. Trapping of electrons in a proton storage ring has been reported in Ref. [5]. Electron trapping has also been observed in the CESR dipole magnets in the electric fields of distributed ion pumps [6]. We report here on the measurement of electron trapping over more than an entire $2.5 \mu\text{s}$ beam revolution period arising from electron cloud buildup in a quadrupole magnet in the CESR ring. Our interest in quantifying electron buildup in a positron damping ring is motivated by the possible operational limitations on the damping rings required for a future high-energy linear $e + e^-$ collider.

The development of time-resolving electron detectors has been shown to provide highly detailed information on local cloud development, allowing the independent characterization of photoelectron and secondary electron production mechanisms [7]. Figure 1 a) shows the circular stainless steel vacuum chamber of inner diameter 95.5 mm in the 60-cm-long quadrupole magnet. Three detectors are placed directly in front of magnet poles, as shown in Fig. 1 b). The detector shown on the lower

right is placed in the fringe field of the magnet; the other two are centrally located. Electrons are collected on the 6-mm-wide copper collector shown in Fig. 1 c). The collector is etched on one side of a 0.12-mm-thick Kapton sheet, forming a transmission line with the grounded copper on the other side. A pattern of 5×60 0.8-mm-diameter parallel holes (see Fig. 1 d) in the beam-pipe allows transmission of cloud electrons to the detector shown on the upper right in Fig. 1 b). This Letter reports solely on measurements obtained with this detector.

The hole diameter was chosen to achieve a depth-to-diameter ratio of 3:1, which effectively shields the detector from the directly induced signal from the beam bunch passages [8]. The hole pattern is 7.1 mm wide and 94.4 mm long and located in front of the rectangular portion of the collector, which is 101.6 mm long. The collector ends are tapered so as to minimize reflections in the signal transmission. The collector was biased with +50 V relative to the vacuum chamber in order to avoid contributions to the signal from secondary electrons escaping the collector surface. This choice of bias provides sensitivity to electrons which enter the holes with low kinetic energy. The front-end readout electronics consists of two Mini-Circuits ZFL-500 broadband amplifiers with 50 Ω input impedance and a total gain of 40 dB. Digitized oscilloscope traces are recorded in 1024 0.5 ns time bins to 8-bit accuracy with auto-scaling, averaging over 8k triggers.

The CESRTA program for April and June of 2013 included electron cloud buildup measurements with shielded pickup detectors, spectrum analyzers for electron-cloud-induced TE-wave sidebands and more than thirty retarding-field-analyzers. Figure 2 shows results from the time-resolving electron detector installed in a quadrupole magnet obtained for 10- and 20-bunch trains of 5.3 GeV positrons. The average bunch populations are 6.6×10^{10} and 1.3×10^{11} for the data shown in Figs. 2 a) and b), respectively. The bunch spacing is 14 ns and the bunch-to-bunch filling uniformity is a few percent. The quadrupole field gradient in these conditions is 7.4 T/m.

The raw oscilloscope signals exhibit beam-induced

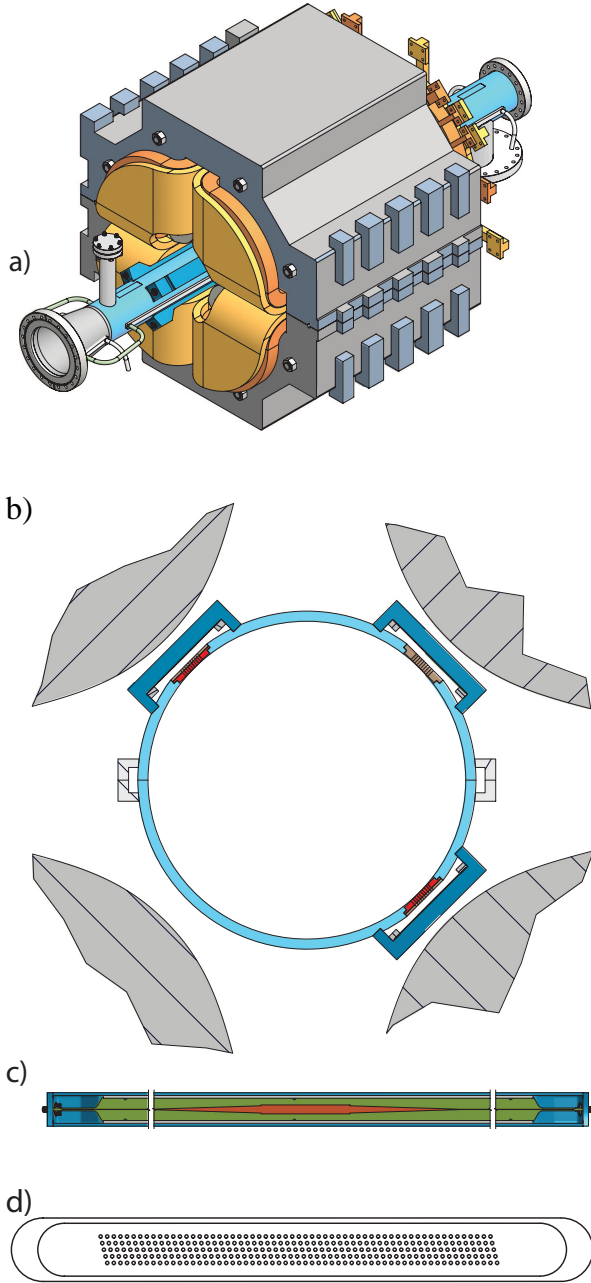


FIG. 1. a) Vacuum chamber equipped with electron detectors in the quadrupole magnet. b) Arrangement of three detectors in front of the magnet poles as seen from the positron arrival direction. c) Geometry of the copper electrode biased at 50 V to collect electrons entering through the pattern of holes in the beam-pipe shown in d). The rectangular region of the collector and the pattern of holes are both about 10 cm long.

noise following the passage of each bunch due to a high-pass bandwidth characteristic of the detector. A 13 MHz low-pass filtering algorithm was applied to the data, suppressing this induced noise by an order of magnitude. The more rapid cloud buildup during the first ten bunches of the 20-bunch train relative to that for the ten-bunch train clearly shows the presence of cloud prior

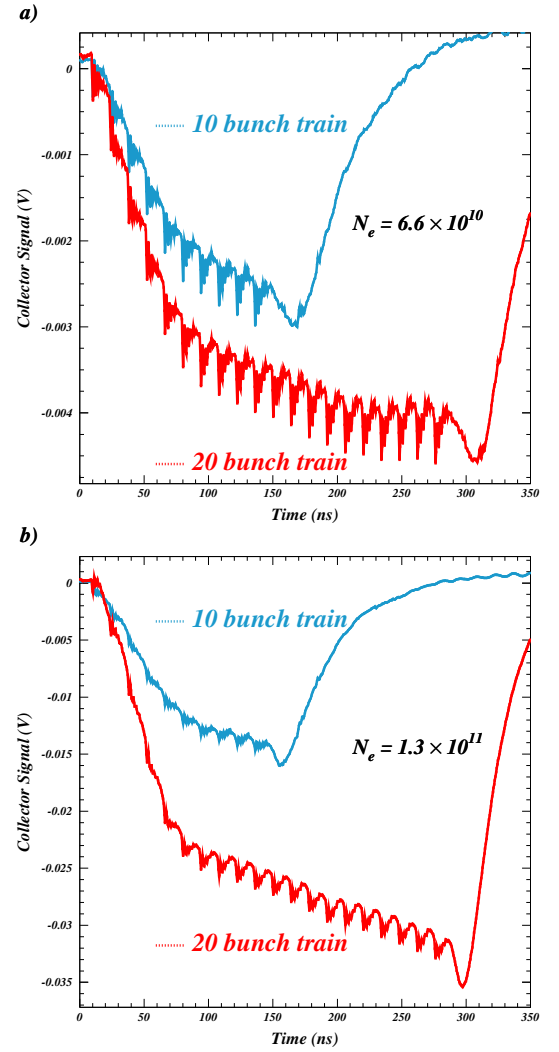


FIG. 2. Electron detector signals recorded for 10- and 20-bunch trains of 5.3 GeV positrons. The average bunch populations are a) 6.6×10^{10} and b) 1.3×10^{11} . Averaged over 8000 revolutions, the enhanced cloud buildup during the first ten bunches of a 20-bunch train relative to that for the 10-bunch train shows that electrons were trapped during the $2.5 \mu\text{s}$ interval between train passages.

to the arrival of the train. The excess charge is due to the buildup of trapped electrons over multiple beam revolutions. One can conclude that the trapping time is at least as long as the CESR revolution time of $2.562 \mu\text{s}$. The trapping increases with bunch population, and the intriguing decrease in cloud buildup rate following the first seven bunches may indicate that a trapped class of electrons which can contribute to the cloud reaching the detector has become depleted at that time. Another interesting feature of the measurements is the increase in signal following the trailing bunch of the train. It corresponds to a region of cloud electron phase space which was prevented by the positron beam from reaching the vacuum chamber surface.

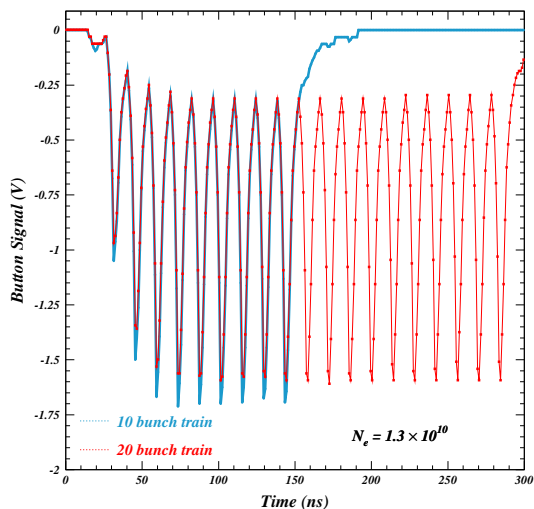


FIG. 3. Electron detector signals recorded with shielded pickup detectors in a field-free region of the ring simultaneously with the measurements shown in Fig. 2 b). No evidence for electron trapping is observed.

Figure 3 shows data recorded simultaneously in these beam conditions with shielded pickup detectors located in sections of the ring with no applied magnetic field. Electron trapping is observed to be less than 1%. The signal for the 20-bunch train is in fact slightly smaller than for the 10-bunch train because the average bunch population was 2% lower.

The long-term trapping of electrons in nonuniform fields such as quadrupoles can be understood based on the presence of an adiabatic invariant which is the magnetic moment associated with the cyclotron motion of the electron. This is given by $\mu = mv_{\perp}^2/2B$ where m is the mass of the electron, B is the magnetic field at that point, and v_{\perp} is the velocity perpendicular to the local magnetic field. This quantity remains an invariant as long as $dB/B \ll 1$ during the cyclotron motion, or equivalently

$$\Gamma = \frac{\nabla B}{B} r_c \ll 1, \quad (1)$$

where r_c is the cyclotron radius. Combining the conditions of conservation of magnetic moment and conservation of energy, one can specify a “velocity-space loss cone” which defines the trapping condition (see, for example, Ref. [9]). A particle moving from a region of lower field to a region of higher field reverses its path if the velocity components perpendicular and parallel to the magnetic field at the starting position, denoted by v_{\perp} and v_{\parallel} respectively, are related such that

$$v_{\parallel}/v_{\perp} \leq 1 - (B_{bd}/B_{in})^{1/2}. \quad (2)$$

Here B_{in} is the magnetic field value at the start point, and B_{bd} is the magnetic field along the field line at the

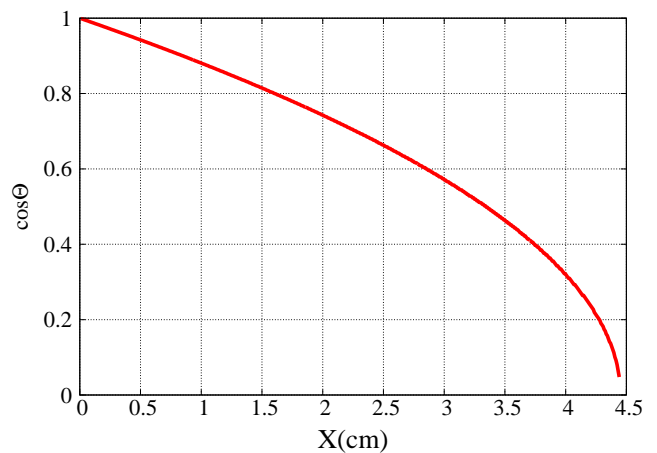


FIG. 4. Cosine of the loss-cone angle vs. horizontal position in the mid-plane of the vacuum chamber

boundary beyond which the particle is considered lost. If the above relationship is satisfied, the particle reaches a point where the parallel velocity goes to zero, and the particle reverses its path along the field line. In a quadrupole magnetic field, the trapped particle is confined between two such turning points located along a field line symmetric about either the horizontal or the vertical axis. While the particle mirrors between the pair of turning points, it drifts in the longitudinal direction until it reaches the fringe region of the quadrupole, where it can escape. This drift is caused by a nonzero gradient and curvature in the magnetic field, often referred to as the “grad B” and “curvature” drift respectively. For the parameters of the experiment reported in this Letter, the longitudinal drift over the duration of one beam revolution is significant only when the electron energy is of the order of 1 keV. The energy distribution obtained from the cloud build-up modeling described below indicate that less than 3% of the electrons have energies exceeding 1 keV.

Figure 4 shows the dependence of cosine of the loss cone angle on horizontal position in the mid-plane of the vacuum chamber. This quantity is given by $\cos \Theta = \sqrt{1 - B_{in}/B_{bd}}$ and represents the fractional solid angle in velocity space within which a particle remains confined. Thus, for a localized distribution of isotropic velocities, it represents the probability of confinement at that point. It is clear that the probability of confinement decreases as the point moves toward the boundary along the horizontal axis. However, it is also necessary that the condition described by Eq. 1 remain satisfied. Otherwise, the motion of the particle is non-adiabatic, for example near the center of the field (beam axis). In such a case, a particle moves to a region of higher magnetic field, bounces back toward the center, and depending on the phase of the cyclotron motion it acquires near the center, may move in a different direc-

tion away from the center. This procedure repeats itself until the particle enters the loss cone and gets lost. The loss occurs along the 45° lines between the pole faces of the quadrupole where the particle is not required to cross field lines and can thus escape. Figure 5 indicates how

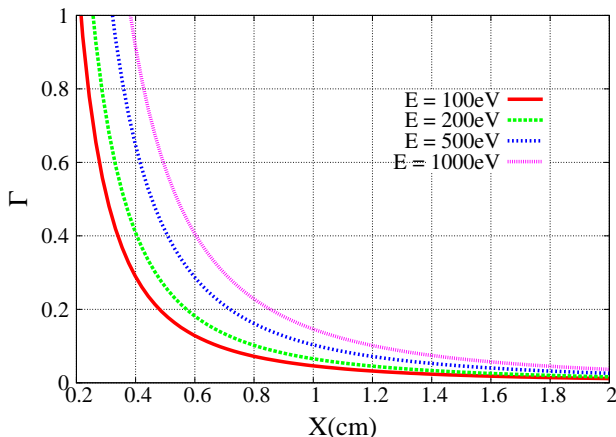


FIG. 5. The quantity $\Gamma = \frac{\nabla B}{B} r_c$ versus horizontal position for various kinetic energies, calculated for a quadrupole field gradient of $7.3T/m$. Trapping requires $\Gamma \ll 1$.

well the condition given by Eq. 1 is satisfied near the center for various energies. Along a horizontal line passing through the center, the quantity Γ is given by

$$\Gamma = \frac{1}{K} \sqrt{\frac{2Em}{e}} \frac{1}{x^2} \quad (3)$$

where K is the quadrupole field gradient, E is the energy in eV and x is the distance along the horizontal axis.

In order to verify that the observation of electron trapping can be expected for our experimental conditions, we have employed the electron cloud buildup modeling program ECLOUD [10]. The code has been under active development for the purposes of CESR-TA since 2008. Developed at CERN in the 1990s, it has seen widespread application for phenomena observed at CERN, KEK, Stanford Linear Accelerator Laboratory, and Brookhaven National Laboratory. It has successfully described the CESR-TA measurements of coherent tune shifts [11], which are sensitive to ring-averaged cloud buildup, as well as local measurements with shielded pickup detectors [7] and time-resolved retarding-field analyzers [12]. The ECLOUD code includes simulation algorithms for photoelectron generation, for time-sliced macroparticle tracking in the 2D electrostatic fields sourced by the beam and the cloud, and for 3D tracking in a variety of ambient magnetic fields, as well as for a detailed model of the interactions of cloud electrons with the vacuum chamber surface producing secondary electrons.

The code has been supplemented with response functions for the CESR-TA time-resolving electron detectors. As a function of incident angle and energy, a fraction of

the macroparticle charge hitting the wall in the region of the detector contributes to the modeled signal. The remaining charge generates secondary electrons. The modeled signal in each time slice thus carries a statistical error associated with the number of contributing macroparticles. The model employed to describe the 10- and 20-bunch trains discussed here generated 4×10^3 macroparticles during the passage of each bunch, each macroparticle carrying thousands of electron charges. The development of the cloud is calculated in 100 time slices during the passage of the 1-cm long bunch, and in 400 time slices between bunch passages. The electric fields due to the cloud space charge and the beam bunch were calculated eleven times both during and between the bunch passages. The amplitude of the modeled signal was very sensitive to the assumed secondary emission yield, increasing by an order of magnitude as the peak secondary yield was increased from 1.4 to 1.9. The measured signal amplitude was reproduced with values for the peak secondary yield and elastic yield [13] of 1.4 and 0.5, respectively.

Figure 6 a) shows the resulting modeled electron cloud density averaged over the volume of the circular, 1-m-long, vacuum chamber for the case of two 10-bunch trains of positrons with bunch population 1.3×10^{11} . The density reaches $2.7 \times 10^{12} \text{ m}^{-3}$ following the first train and falls to $1.4 \times 10^{11} \text{ m}^{-3}$ after a few hundred nanoseconds. This residual cloud is trapped until the bunch train returns. Figure 6 b) shows the model result for the field-free region equipped with shielded pickup detectors under the same beam conditions.

The modeled transverse distribution of the cloud trapped in the quadrupole magnet is shown in Fig. 7 at a time immediately preceding the return of the train. The mirroring electrons are concentrated in four quadrants near the beam outside of a central depletion zone of 2 cm radius and in the horizontal plane close to the vacuum chamber walls. The median energy of the trapped electrons was found to be about 50 eV. It is notable that since no electrons survive in the diagonal escape zones until the end of the revolution time, the signal produced by the trapped cloud requires several bunch passages (in these conditions about seven) to accelerate the available trapped electrons into the escape regions of phase space. We also verified that removing the quadrupole magnetic field from the ECLOUD model resulted in the trapped cloud density falling to less than 0.1%.

In summary, recent measurements with a novel time-resolving electron detector located in a quadrupole magnetic field have provided comparisons of signals from 10- and 20-bunch trains of positrons which show clear evidence for electron trapping during the entire $2.5 \mu\text{s}$ revolution time of the storage ring. Modeling tuned to the recorded signals indicates that approximately 5% of the cloud generated by a 5.3 GeV train of bunches each carrying 1.3×10^{11} positrons remains trapped. These and future measurements in the CESR-TA program will inform

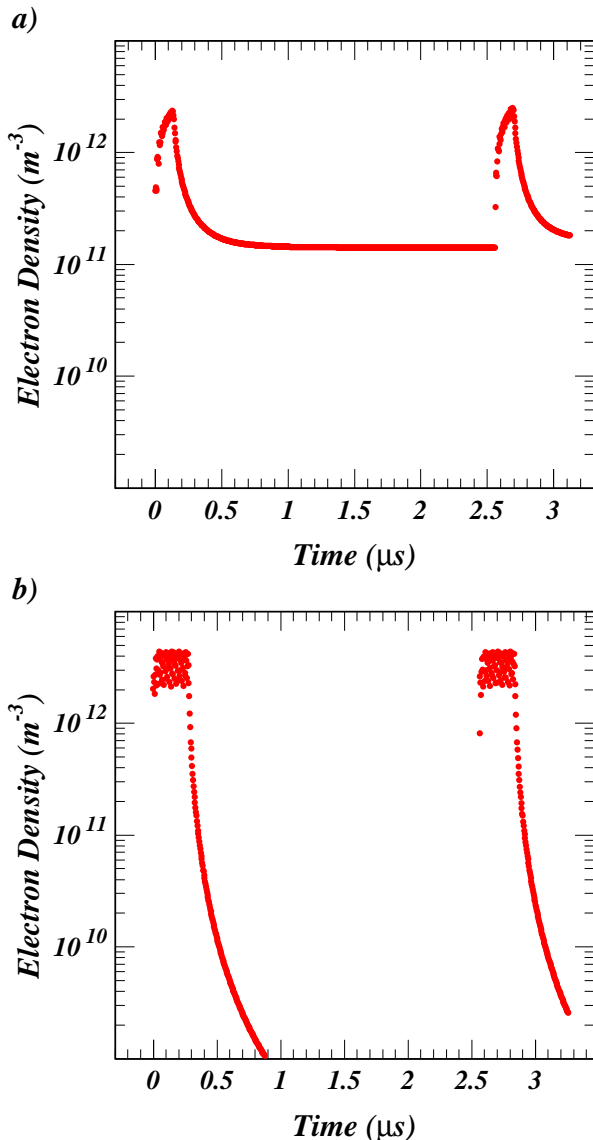


FIG. 6. Results from the numerical model of electron buildup in the quadrupole magnet for the case of a 5.3 GeV 10-bunch train of positrons, each bunch carrying 1.3×10^{11} positrons. a) The time dependence of the modeled cloud density indicates that about 5% of the cloud generated by passage of the first train is trapped for an entire beam revolution. b) The cloud density modeled in the field-free region equipped with shielded pickup detectors for the same beam conditions.

studies of mitigation techniques serving the goal of raising beam current limitations on high-energy linear collider damping rings.

ACKNOWLEDGMENTS

We wish to thank Joe Calvey, Gerry Dugan and Miguel Furman for useful discussions.

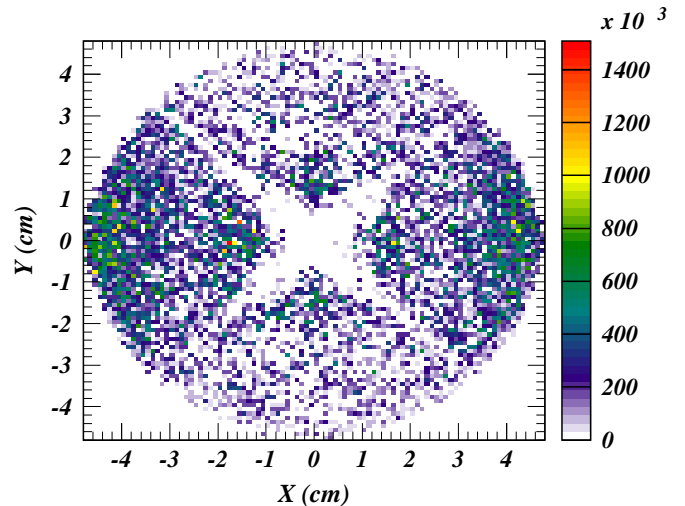


FIG. 7. The modeled transverse distribution of the trapped cloud shown at the end of the first beam revolution. The color scale ranges up to a maximum of 1.4×10^6 electrons/bin.

-
- [1] G.F. Dugan, M.A. Palmer, and D.L. Rubin, *ILC Damping Rings R&D at CESRTA*, ICFA Beam Dynamics Newsletter Nr. 50, eds. J. Urakawa and W. Chou (2009)
 - [2] F. Zimmerman, *Electron-Cloud Effects in Past and Future Machines - Walk Through 50 Years of Electron-Cloud Studies*, ECLOUD'12, Joint INFN-CERN-EuCARD-AccNet Workshop on Electron-Cloud Effects, La Biodola, Isola d'Elba, Italy, 5-9 June 2012; CERN-2013-002, pp. 9-17
 - [3] K. Ohmi, *Beam-Photoelectron Interactions in Positron Storage Rings*, Phys. Rev. Lett. **75**, 1526 (1995)
 - [4] M.A. Furman and G.R. Lambertson, *The Electron-Cloud Instability in PEP-II: An Update*, proceedings of PAC97, Vancouver, BC, Canada (1997)
 - [5] R.J. Macek *et al.*, *Electron Cloud Generation and Trapping in a Quadrupole Magnet at the Los Alamos Proton Storage Ring*, Phys Rev ST-AB **1**, 010101 (2008)
 - [6] T. Holmquist and J.T. Rogers, *A Trapped Photoelectron Instability in Electron and Positron Storage Rings*, Phys. Rev. Lett. **79**, 3186 (1997)
 - [7] J.A. Crittenden and J.P. Sikora, *Electron Cloud Buildup Characterization Using Shielded Pickup Measurements and Custom Modeling Code at CESRTA*, ECLOUD'12, Joint INFN-CERN-EuCARD-AccNet Workshop on Electron-Cloud Effects, La Biodola, Isola d'Elba, Italy, 5-9 June 2012; CERN-2013-002, pp. 241-250
 - [8] M. Sands, *Energy Loss from Small Holes in the Vacuum Chamber*, PEP-253, (1977)
 - [9] *Introduction to Plasma Physics*, R.J. Goldstone and P.H. Rutherford, IOP Publishing (2003)
 - [10] F. Zimmermann, G. Rumolo and K. Ohmi, *Electron Cloud Build Up in Machines with Short Bunches*, ICFA Beam Dynamics Newsletter Nr. 33, eds. K. Ohmi & M. Furman (2004).
 - [11] J.A. Crittenden *et al.*, *Progress in Studies of Electron-Cloud-Induced Optics Distortions at CESRTA*, proceed-

- ings of IPAC10, Kyoto, Japan (2010)
- [12] J.A. Crittenden *et al.*, *Modeling for Time-Resolved Retarding-Field Analyzer Measurements of Electron Cloud Buildup at CESR-TA*, proceedings of IPAC13, Shanghai, China (2013)
- [13] M.A. Furman and M.T.F. Pivi, *Probabilistic Model for the Simulation of Secondary Electron Emission*, Phys Rev ST-AB 5, 124404 (2002)